PHYSICAL FOUNDATIONS
OF STRENGTH AND PLASTICITY

Local State of Stress of the Material at the Crack Tip for Various Types of Loading

G. V. Klevtsov[a], *, R. Z. Valiev[b], N. A. Klevtsova[a], A. M. Glezer[c], and I. N. Pigaleva[a]

[a] Togliatti State University, Togliatti, 445667 Russia
[b] Ufa State Aviation Technical University, Ufa, 450000 Russia
[c] Bardin Central Research Institute for Ferrous Metallurgy, Moscow, 105005 Russia
*e-mail: klevtsov11948@mail.ru

Abstract—The parameter h_{max}/t (where h_{max} is the maximum depth of the plastic zone under the fracture surface, t is the specimen or part thickness) estimated by X-ray diffraction is shown to be used as a general criterion for the local state of stress of the material at the crack tip during static, impact, and cyclic loading of coarse-grained and ultrafine-grained materials.

INTRODUCTION

The estimation of the local state of stress (SOS) of the material at the crack tip is of fundamental importance, e.g., on testing materials for static fracture toughness (K_{Ic}) under plane-strain (PSN) conditions [1–3]. This fully applies both to coarse-grained (CG) materials and to a new class of structural materials, namely, ultrafine-grained (UFG) materials fabricated by severe plastic deformation [4–8].

The estimation of the local SOS of a material on diagnosing the causes of accidental fracture of structures and machine parts is also important; for this purpose, it is necessary to observe similarity in the local SOS of a material in a destroyed part and a simulating specimen [9–11]. The destruction of structures and machine parts can occur both in single (static, impact) and with cyclic types of loading; therefore, a general criterion for estimating the local SOS of materials for single and cyclic types of loading is necessary.

According to fracture mechanics, the most objective information about the local SOS of a material at fracture is provided by an analysis of the size and shape of the plastic zones formed at the crack tip [1, 3, 12]. In fracture mechanics, the following two limiting local SOSs of a material are distinguished: plain-strain (PSN) and plain-stress (PSS) states [1, 3, 12]. However, in practice, the destruction of metal materials often occurs in a transition region (PSN ↔ PSS) [7, 11].

PSN state is considered to take place when the well-known fracture mechanics criterion

$$t/(K/\sigma_{0.2})^2 \geq 2.5,$$

where t is the specimen thickness and $\sigma_{0.2}$ is the yield strength, is met [2, 3].

There is also the following relation between the radius of the plastic zone at the crack tip r_y and the ratio $(K_I/\sigma_{0.2})^2$ [3]:

$$r_y = \frac{1}{\pi n}\left(\frac{K_I}{\sigma_{0.2}}\right)^2, \qquad (1)$$

where coefficient n depends on the local SOS of the material at the crack tip. As coefficient n increases, the constraint of plastic deformation increases and the PSS → PSN transition occurs.

The authors of [10, 13, 14] proposed a modification of the criterion of the local SOS of a material in the form of the ratio h_{max}/t, where h_{max} is the maximum depth of the plastic zone under the fracture surface and t is the specimen or part thickness. Parameter h_{max} is estimated by an X-ray diffraction method; therefore, it can be determined for any type of loading of a specimen or part, which is the main advantage of the criterion h_{max}/t over the criterion $t/(K/\sigma_{0.2})^2$. During static loading under PSN conditions, we have $h_{max}/t < 10^{-2}$ due to the small plastic zone size because of severe constraint of the material. Under PSS conditions, fracture is accompanied by the formation of two plas-

tic zones: a strongly deformed microzone of depth h_{yh} and a weakly deformed macrozone of depth h_y. We have $h_{max}/t > 10^{-1}$ due to large size h_y of the macrozone under PSS conditions. In the transition zone (PSN $\leftrightarrow$ PSS), we have $10^{-2} \le h_{max}/t \le 10^{-1}$ [10, 13, 14].

The comparison [15] of the criterion h_{max}/t with the well-known criterion for meeting PSN conditions $t/(K_{1c}/\sigma_{0.2})^2 \ge 2.5$ [2] for static fracture toughness (K_{1c}) tests of CG and UFG materials demonstrated that the criterion $t/(K_{1c}/\sigma_{0.2})^2 \ge 2.5$ is less stringent than the criterion $h_{max}/t < 10^{-2}$ and extends to part of the transition region (PSN $\leftrightarrow$ PSS). When determining PSN conditions according to ratio $t/(K_{1c}/\sigma_{0.2})^2$, it is necessary to take into account the type of crystal lattice. For bcc materials, the PSN condition is fulfilled at $t/(K_{1c}/\sigma_{0.2})^2 \ge 5$, for fcc and hcp materials, this condition is met at $t/(K_{1c}/\sigma_{0.2})^2 \ge 10$, which corresponds to $h_{max}/t < 10^{-2}$ [15].

The purpose of this work was to substantiate the possibility of using the ratio h_{max}/t as a criterion for estimating the local SOS of the material at the crack tip in both CG and UFG materials for various types of loading.

EXPERIMENTAL

We studied the following metallic materials with various types of lattices and in various structural states:

materials with bcc lattice: carbon steels 10 (0.1% C), 20 (0.2% C) and 45 (0.45% C) and 09G2S alloy steel (0.09% C, 0.64% Si, 1.26% Mn, 0.1% Ni, 0.08% Cr, 0.14% Cu, 0.02% Al);

materials with fcc lattice: aluminum alloys D16 (4.5% Cu, 0.6% Mn, 0.2% Si, 1.5% Mg, 0.12% Zn, 0.23% Fe) and AK4-1 (2.46% Cu, 1.48% Mg, 0.89% Fe, 0.22% Si, 0.92% Ni, 0.04% Mn, 0.04% Ti), austenitic steels 40Kh4G18F (0.43% C, 4.2% Cr, 18.0% Mn, 1.41% V), 07Kh13N4AG20 (0.06% C, 21.87% Mn, 14.86% Cr, 4.89% Ni, 45% Si, 0.14% N) and AISI 321 (0.08% C, 17.85% Cr, 7.35% Ni, 0.39% Mo, 0.55% Si);

materials with hcp lattice: titanium alloys VT6 (5.95% V, 5.01% Al) and VT8M-1 (5.7% Al, 3.8% Mo, 1.2% Zr, 1.3% Sn, 0.16% Fe) and Mg6Al magnesium alloy (5.6% Al, 0.245% Mn, 0.047% Cl, 0.046% Ca).

The materials were studied in a CG state after heat treatment and in a UFG state after severe plastic deformation of various types (Table 1). To reach a UFG state, grade 10 steel was water quenched after annealing from a temperature of 880°C, and the billets were then subjected to equal-channel angular pressing (ECAP) at a temperature of 200°C (route Bc is the rotation of a workpiece through 90°, the number of passes is $n = 6$, the angle of intersection of the die channels is $\varphi = 120°$) [7, 8]. Grade 45 steel was water quenched from 800°C and tempered at 350°C, and the billets were then subjected to ECAP at 350°C (route Bc, $n = 6$, $\varphi = 120°$).

The processing of 09G2S steel included homogenizing annealing at 820°C, water quenching, subsequent tempering at 350°C, ECAP at 350°C (route Bc, $n = 4$, $\varphi = 120°$), and additional annealing at 350°C for 10 min. Austenitic AISI 321 steel was subjected to ECAP at 400°C (route Bc, $n = 4$, $\varphi = 120°$). ECAP of AK4-1 aluminum alloy was carried out at 160°C after quenching (route Bc, $n = 6$, $\varphi = 90°$).

The UFG state of the VT6 alloy was achieved by ECAP or ECAP with subsequent isothermal upsetting (IU). Before ECAP, homogenizing annealing was performed with water quenching from a temperature of 960°C followed by tempering at 675°C for 4 h; ECAP was performed at 650°C (route Bc, $n = 6$, $\varphi = 120°$). After ECAP, some billets were subjected to IU up to $\varepsilon = 30\%$ at a temperature of 750°C and a strain rate of 10^{-2} s^{-1}.

The UFG state of the VT4-1 alloy was achieved by water quenching from a temperature of 940°C followed by annealing at 700°C for 1 h and cooling in air; as a result, a globular-plate structure was formed. The billet was then subjected to rotary forging (RF) at a temperature of 750°C; (true strain was $e \approx 1.7$, strain rate is higher than 300 mm s^{-1}) [8]. Before ECAP of Mg6Al alloy, annealing was performed at 430°C for 24 h in an argon atmosphere, and ECAP was performed at 400°C (route Bc, $n = 4$, $\varphi = 120°$) with intermediate annealing at 400°C for 15 min.

The average grain sizes and the mechanical properties of the materials after various types of treatment are given in Table 1.

CG and UFG material specimens were subjected to impact toughness (KCV) tests in the temperature range from 150 to −196°C. Fatigue tests were carried out according to the three-point bending scheme (steel 45, Mg6Al alloy) and the off-center tension scheme (D16 alloy; 20, 45, 07Kh13H4AG20 steels) at various temperatures, loads (ΔP, P_{max}), and stress ratios (R).

To determine the plastic zone depths under the fracture surfaces, we used layer-by-layer etching followed by X-ray diffraction (XRD) analysis of the surfaces (method is described in detail in [10, 16−18]). The total error in determining the plastic zone depths by the XRD method is, as a rule, 10−30% and depends on the type of fracture [16]. The error increases more than twice [16] when the fracture surfaces formed under conditions close to plane deformation are studied, when

Table 1. Average grain size and the mechanical properties of the materials after treatment under various conditions

Material	Type of treatment	d_{av}, μm	σ_u, MPa	$\sigma_{0.2}$, MPa	δ, %
Steel 20	Annealing	55	450	260	24
Steel 45	Annealing	75	590	320	20
09G2S	Hot rolling	15	485	354	40
40Kh4G18F	Quenching	75	900	400	55
07Kh13N4AG20	Quenching	50	685	365	62
AK4-1	Quenching + aging	40	503	399	13
D16	Hot rolling	–	233	117	12
VT6	Hot rolling	–	950	849	12
VT8M-1	Hot rolling	–	1017	949	16
Steel 10	ECAP	0.3	1028	989	8
Steel 45	ECAP	0.56	1171	1064	5
09G2S	ECAP	0.6	838	461	13
AISI 321	ECAP	0.3	917	869	25
AK4-1	ECAP	0.3	533	489	7
VT6	ECAP	0.24	1090	990	8
VT6	ECAP + IU	0.56	1100	1090	8
VT8M-1	RF	0.3	1216	1137	11
Mg6Al	ECAP	20	260	100	10

the plastic zone depth is comparable with the thickness of the effectively scattering material layer [10, 19].

RESULTS AND DISCUSSION

As was shown in [7, 10], the formation of plastic zones at the crack tip during impact loading is the same as that during static loading; therefore, there are no fundamental restrictions on the use of the criterion h_{max}/t for estimating the local SOS of a material under dynamic load. In the absence of an opportunity to compare the PSN criteria h_{max}/t and $t/(K/\sigma_{0.2})^2 \geq 2.5$ for impact loading, for this purpose we use another criterion, namely, the relative reduction of area of specimens ($\psi_c < 1.5\%$) [2], which is applied to estimate the fracture toughness under static loading. As follows from the data obtained, the relative reduction of areas of all impact specimens and the specimens subjected to K_{1c} tests under PSN conditions (according to the criterion $h_{max}/t < 10^{-2}$) do not exceed 1.5% (Fig. 1). Based on this finding, we can assume that the criterion h_{max}/t is effective for estimating the local SOS of the material at the crack tip not only under static, but also under impact loading of CG and UFG materials.

Currently, fracture mechanics has no criterion characterizing the local SOS of the material at the tip of a fatigue crack [3, 12, 20]. We now consider the possibility of applying the criterion h_{max}/t for this purpose. It is known that, during cyclic loading of metallic materials, the following two plastic zones form at the tip of a fatigue crack according to the theoretical Rice model [21]: monotonic zone h_y associated with maximum tensile stresses, and cyclic zone h_{yh} caused by reverse plastic deformation (Fig. 2). In this case, parameter h_y correlates well with the maximum stress intensity factor K_{max}, and parameter h_{yh}, with the range of the coefficient ΔK [10]. As the fatigue crack length increases (coefficients ΔK and K_{max} increase), the plastic zone depths h_{yh} and h_y under the fatigue fracture surface also increase (see Fig. 2b). Therefore, the local SOS of the material at the crack tip is assumed to change toward plane SOS [10].

By its nature, the monotonic plastic zone of depth h_y is similar to the weakly deformed macrozone for single types of loading, since it forms at the maximum cycle stress σ_{max} [3, 20, 22]. Therefore, we write the ratio $t/(K_I/\sigma_{0.2})^2$ as $t/(K_{max}/\sigma_{0.2})^2$ for the case of cyclic loading [10]. The results of tests performed at various temperatures under various cyclic loading conditions for a wide range of CG and UFG materials with bcc, fcc, and hcp lattices indicate that this criterion is
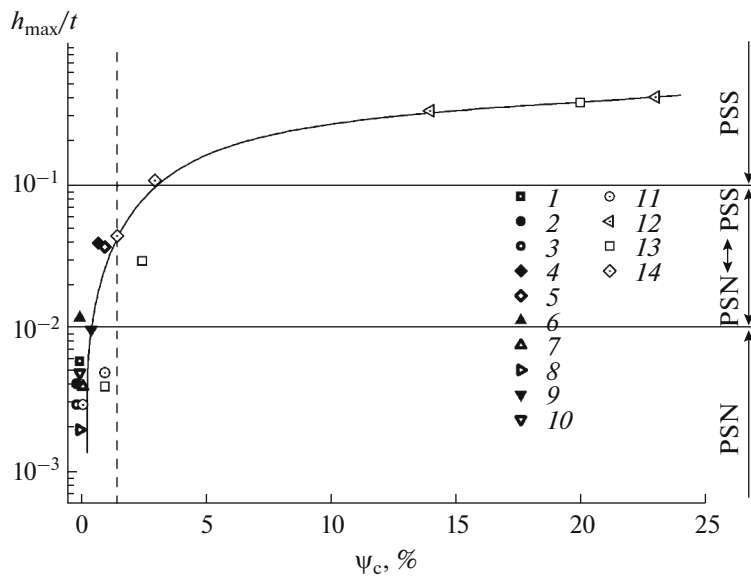
Fig. 1. Relation between the criterion h_{max}/t and the relative reduction of area ψ_c near the fracture surfaces of CG and UFG specimens (*1–3*, *11*) bcc, (*4*, *5*, *12–14*), fcc, and (*6–10*) hcp lattices. The vertical dotted line bounds the range $\psi_c \leq 1.5\%$ for PSN conditions. (solid symbols) Static K_{Ic} tests, (open symbols) impact tests (KCV). CG materials: (*2*) 09G2S steel, (*4*) AK4-1 alloy, (*6*) VT6 alloy (*9*) VT8M-1 alloy, and (*13*) 40Kh4G18F steel. UFG materials: (*1*) steel 45 (ECAP), (*3*) steel 09G2S (ECAP), (*5*) AK4-1 alloy (ECAP), (*7*) VT6 alloy (ECAP), (*8*) VT6 alloy (ECAP + IU), (*10*) VT8M-1 alloy (RF), (*11*) steel 10 (ECAP), (*12*) steel AISI (ECAP), and (*14*) AK4-1 alloy (ECAP).
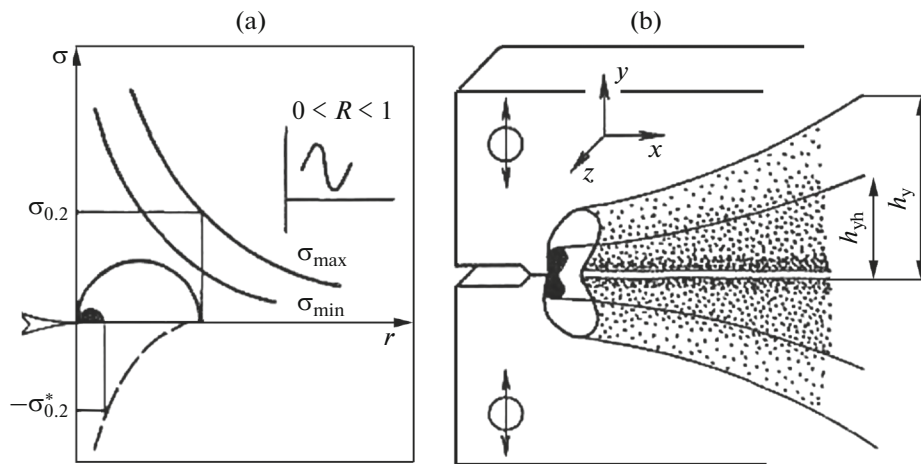

Fig. 2. (a) Scheme of plastic zone formation at the tip of a fatigue crack and (b) changes in the plastic zone depths under the surface of fatigue fracture: r is the radius of a plastic zone at the tip of a fatigue crack, h_y is the depth of the monotonic plastic zone (bright area), h_{yh} is the depth of the cyclic plastic zone (dark area), and $\sigma_{0.2}^{*}$ is yield strength of the material under compression.

related to the criterion h_{max}/t, wherfe h_{max} is the the monotonic plastic zone depth (Fig. 3). It should be noted that most studied materials, including those with a bcc lattice, undergo fracture in the transition region (PSN $\leftrightarrow$ PSS) during fatigue loading, which is unusual for bcc materials and single types of loading

[10]. The data in Fig. 3 allow us to conclude that the PSN condition is met at $t/(K_{max}/\sigma_{0.2})^2 > 3.0$ during cyclic loading of specimens.

Thus, the criterion h_{max}/t can be used to estimate the local SOS at the crack tip in CG and in UFG materials not only for single types of loading (impact,
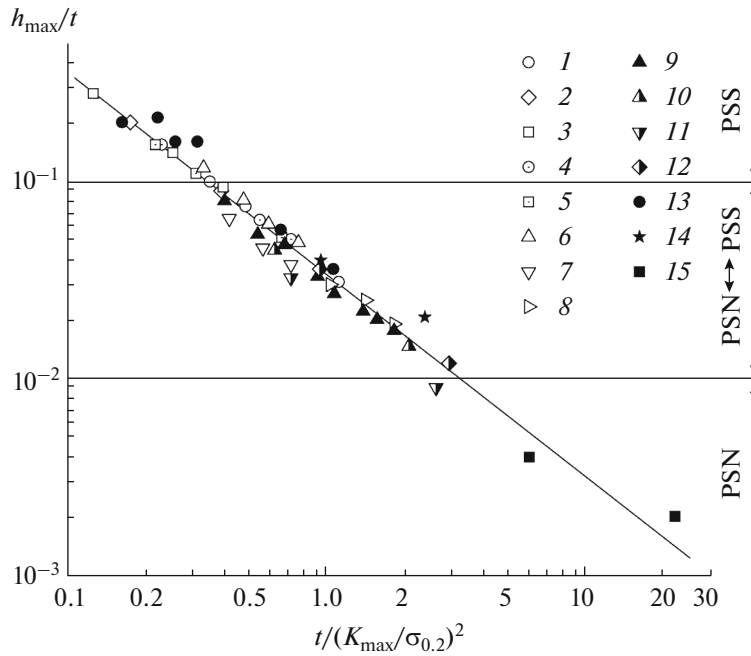
Fig. 3. Relation between the criteria h_{max}/t and $t/(K_{max}/\sigma_{0.2})^2$ during cyclic loading for materials with (*9, 13, 15*) bcc, (*1–8, 10–12*), fcc, and (*14*) hcp lattices: CG-materials: (*1*) D16 alloy ($t = 10^{-2}$ m, $R = 0.1$, $\Delta P = $ const), (*2*) D16 alloy ($t = 10^{-2}$ m, $R = 0.3$, $\Delta P = $ const), (*3*) D16 alloy ($t = 10^{-2}$ m, $R = 0.5$, $\Delta P = $ const), (*4*) D16 alloy ($t = 10^{-2}$ m, $R = 0.1$, $P_{max} = $ const), (*5*) D16 alloy ($t = 10^{-2}$ m, $R = 0.5$, $P_{max} = $ const), (*6*) D16 alloy ($t = 1.5 \times 10^{-2}$ m, $R = 0.5$), (*7*) D16 alloy ($t = 3 \times 10^{-2}$ m, $R = 0.5$), (*8*) D16 alloy ($t = 5 \times 10^{-2}$ m, $R = 0.5$), (*9*) steel 20 ($t = 2 \times 10^{-2}$ m, $R = 0.5$), (*10*) 07Kh13N4AG20 steel ($t = 2 \times 10^{-2}$ m, $R = 0.5$, $T = 20°C$), (*11*) 07Kh13N4AG20 steel ($t = 2 \times 10^{-2}$ m, $R = 0.5$, $T = -80°C$), (*12*) 07Kh13N4AG20 steel ($t = 2 \times 10^{-2}$ m, $R = 0.5$, $T = -196°C$), and (*13*) steel 45 (impact-cyclic loading, $t = 1.2 \times 10^{-2}$ m, $R = 0$, $T = 20°C$); UFG-materials: (*14*) Mg6Al alloy (ECAP, $t = 10^{-2}$ m, $R = 0.1$, $T = 20°C$, $\Delta P = $ const) and (*15*) steel 45 (ECAP, $t = 10^{-2}$ m, $R = 0.1$, $T = 20°C$, $\Delta P = $ const).

static), but also for cyclic loading of specimens, structures, and machine parts irrespective of the state of material and the type of crystal lattice.

CONCLUSIONS

(1) The criterion h_{max}/t (h_{max} is the maximum depth of the plastic zone under the fracture surface, t is the specimen or part thickness) can be used to estimate the local SOS at the crack tip in CG and UFG materials for single (static, impact) and cyclic types of loading. For single types of loading in the case of plane SOS and transition state PSN $\leftrightarrow$ PSS, h_{max} is the depth of a weakly deformed macrozone; in the case of cyclic loading, h_{max} is the depth of a monotonic zone.

(2) When materials undergo fracture under PSN conditions, we have $h_{max}/t < 10^{-2}$; when they fail under PSS conditions, we have $h_{max}/t > 10^{-1}$; in the transition region (PSN $\leftrightarrow$ PSS), $10^{-2} \leq h_{max}/t \leq 10^{-1}$.

(3) The PSN condition at the tip of a fatigue crack is met at $t/(K_{max}/\sigma_{0.2})^2 \geq 3.0$ regardless of the state of material, the type of crystal lattice, and loading conditions.

REFERENCES

1. W. Brown and J. Rowley, *Fracture Toughness Testing of High-Strength Metallic Materials under Plane Deformation* (Mir, Moscow, 1972).

2. *GOST 25.506–85. Strength Calculations and Tests. Methods of Mechanical Testing of Metals. Determination of the Fracture Toughness Characteristics under Static Loading* (Izd. Standartov, Moscow, 1985).

3. D. Broek, *Fundamentals of Fracture Mechanics* (Vyshaya Shkola, Moscow, 1980).

4. A. Hohenwarter and R. Pippan, "Fracture toughness and fatigue crack propagation measurements in ultrafine grained iron and nickel. Plasticity, failure, and fatigue," in *Proceedings of Mughrabi Honorary Symposium on Structural Materials—From Macro to Nano* (Minerals, Metals & Materials Society, 2008), pp. 183−188.

5. A. Hohenwarter and R. Pippan, "Fracture of ECAP-deformed iron and the role of extrinsic toughening mechanisms," Acta Mater. **61**, 2973−2983 (2013).

6. F. Wetscher, R. Stock, and R. Pippan, "Fracture processes in severe plastic deformed rail steels," in *Proceedings of 16th European Conference on Fracture* (Alexandroupolis, 2006), pp. 1−9.

7. G. V. Klevtsov, E. V. Bobruk, I. P. Semenova, N. A. Klevtsova, and R. Z. Valiev, *Strength and Fracture Mechanisms of Bulk Nanostructured Metallic Materials* (RIK UGATU, Ufa, 2016).

8. R. Z. Valiev, A. P. Zhilyaev, and T. G. Langdon, *Bulk Nanostructured Materials: Fundamentals and Applications* (Wiley-Blackwell, 2014).

9. A. J. McEvily, *Metal Failures: Mechanisms, Analysis, Prevention* (Wiley InterScience, New York, 2002).

10. G. V. Klevtsov, L. R. Botvina, N. A. Klevtsova, and L. V. Limar, *Fractodiagnostics of the Fracture of Metallic Materials and Structures* (MISiS, Moscow, 2007).

11. M. A. Balter, A. P. Lyubchenko, S. I. Aksenova, A. A. Chernyakova, L. Ya. Gol'shtein, and E. A. Kurits, *Fractography—A Means of Diagnostics of Destroyed Parts* (Mashinostroenie, Moscow, 1997).

12. L. S. Moroz, *Mechanics and Physics of Deformation and Fracture of Materials* (Mashinostroenie, Leningrad, 1984).

13. G. V. Klevtsov and L. R. Botvina, "Plastic deformation macro- and microzone as a criterion of the limiting state of a material during fracture," Probl. Prochn., No. 4, 24−28 (1984).

14. *R 50-54-52/2-94. Strength Calculations and Tests. X-ray Diffraction Analysis of Fracture Surfaces. Determination of the Fracture Characteristics of Metallic Materials by X-ray Diffraction* (VNIINMASh of Gosstandart of Russia, Moscow, 1994).

15. G. V. Klevtsov, R. Z. Valiev, N. A. Klevtsova, I. P. Semenova., I. N. Pigaleva, and M. L. Linderov, "Local stress state of materials with an hcp lattice and plastic zones under the fracture surface," Lett. Mater. **10** (1), 16−21 (2020).

16. *R 50-54-52-88. Strength Calculations and Tests. X-ray Diffraction Analysis of Fracture Surfaces. Determination of the Plastic Deformation Zone Depths under Fracture Surface* (VNIINMASh of Gosstandart of Russia, Moscow, 1988).

17. A. V. Vikulin, V. A. Veselov, M. N. Georgiev, and N. Ya. Mezhova, "Use of X-ray diffraction fractography for the evaluation of fracture toughness of structural materials," Fiziko-Khim. Mekhan. Mater. **20** (5), 98−100 (1984).

18. M. Clavel, D. Fournier, and A. Pineau, "Plastic zone sizes in fatigued specimens of INCO 718," Metall. Mater. Trans. A **6** (12), Article no. 2305 (1975).

19. Ya. S. Umanskií, Yu. A. Skakov, A. N. Ivanov, and L. N. Rastorguev, *Crystallography, X-ray Diffraction, and Electron Microscopy* (Metallurgiya, Moscow, 1982).

20. D. Taylor, "The theory of critical distances," Eng. Fract. Mech. **75**, 1696−1705 (2008).

21. J. R. Rice, "Mechanics of crack tip deformation and extension by fatigue," in *Fatigue Crack Propagation*, Ed. by J. Grosskreutz (ASTM International, West Conshohocken, 1967), pp. 247−311.

22. Y. Murakami, T. Nomoto, and T. Ueda, "Factors influencing the mechanism of super-long fatigue failure in steels," Fatigue Fract. Eng. Mater. **22** (7), 581−590 (1999).

Translated by K. Shakhlevich